




Article

InGaN Resonant-Cavity Light-Emitting Diodes with Porous and Dielectric Reflectors

Cheng-Jie Wang ¹, Ying Ke ¹, Guo-Yi Shiu ¹, Yi-Yun Chen ¹, Yung-Sen Lin ², Hsiang Chen ³
and Chia-Feng Lin ^{1,*}

- ¹ Department of Materials Science and Engineering, Innovation and Development Center of Sustainable Agriculture, Research Center for sustainable energy and Nanotechnology, National Chung Hsing University, Taichung, 145 Xingda Rd., South Dist., Taichung City 402, Taiwan; flyfeeling0101@gmail.com (C.-J.W.); kencookie77@gmail.com (Y.K.); x77889927@hotmail.com (G.-Y.S.); singyi.sky@gmail.com (Y.-Y.C.)
- ² Department of Chemical Engineering, Feng Chia University, Seatwen, Taichung 407, Taiwan; yslin@fcu.edu.tw
- ³ Department of Applied Materials and Optoelectronic Engineering, National Chi Nan University, No.1, University Rd., Puli Township, Nantou County 545, Taiwan; hchen@ncnu.edu.tw
- * Correspondence: cflin@dragon.nchu.edu.tw; Tel.: +886-4-22840500 (ext. 706)

Featured Application: Over the last decades, InGaN-based light-emitting diodes and laser diodes have been widely studied to improve quantum efficiency. However, few studies have focused on the directional emission properties in the short (1λ) InGaN resonant-cavity structure with the porous GaN reflector. The epitaxial 20-period n^+ -GaN/n-GaN stacked structure was transformed into the porous-GaN/n-GaN distributed Bragg reflector (DBR) structure through a simple wet etching process. Directional emission pattern and narrow linewidth were observed in the InGaN active layer with bottom porous DBR, top dielectric DBR, and the optimum Ta₂O₅ spacer layer to match the short cavity structure. We believe that this work can offer a new perspective for the conventional III-V semiconductor community and the readers with the background of the LED and laser.

Abstract: InGaN based resonant-cavity light-emitting diode (RC-LED) structures with an embedded porous-GaN/n-GaN distributed Bragg reflector (DBR) and a top dielectric Ta₂O₅/SiO₂ DBR were demonstrated. GaN:Si epitaxial layers with high Si-doping concentration (n^+ -GaN:Si) in the 20-period n^+ -GaN/n-GaN stacked structure were transformed into a porous-GaN/n-GaN DBR structure through the doping-selective electrochemical wet etching process. The central wavelength and reflectivity were measured to be 434.3 nm and 98.5% for the porous DBR and to be 421.3 nm and 98.1% for the dielectric DBR. The effective 1λ cavity length at 432nm in the InGaN resonant-cavity consisted of a 30 nm-thick Ta₂O₅ spacer and a 148 nm-thick InGaN active layer that was analyzed from the angle-resolved photoluminescence (PL) spectra. In the optical pumping PL spectra, non-linear emission intensity and linewidths reducing effect, from 6.5 nm to 0.7 nm, were observed by varying the laser pumping power. Directional emission pattern and narrow linewidth were observed in the InGaN active layer with bottom porous DBR, top dielectric DBR, and the optimum spacer layer to match the short cavity structure.

Keywords: InGaN; resonant-cavity light-emitting diode; distributed bragg reflector (DBR)



Citation: Wang, C.; Ke, Y.; Shiu, G.; Chen, Y.; Lin, Y.; Chen, H.; Lin, C. InGaN Resonant-Cavity Light-Emitting Diodes with Porous and Dielectric Reflectors. *Appl. Sci.* **2021**, *11*, 8. <https://dx.doi.org/10.3390/app11010008>

Received: 10 November 2020

Accepted: 19 December 2020

Published: 22 December 2020

Publisher's Note: MDPI stays neutral with regard to jurisdictional claims in published maps and institutional affiliations.



Copyright: © 2020 by the authors. Licensee MDPI, Basel, Switzerland. This article is an open access article distributed under the terms and conditions of the Creative Commons Attribution (CC BY) license (<https://creativecommons.org/licenses/by/4.0/>).

1. Introduction

Nitride-based materials are widely used in optoelectronic devices such as light-emitting diodes (LEDs), laser diodes (LDs), and vertical cavity surface emitting lasers (VCSELs) [1,2]. The VCSEL devices have low threshold current density, high efficiency, directional emission pattern, and the ability of high-speed operation properties for the high-density optical storage, biochemical sensors, and micro-projectors. For the short-wavelength VCSEL structures, the InGaN cavity length and the distributed Bragg reflectors

(DBRs) should be considered. In short-wavelength VCSEL, the modulation of the cavity length may suppress the constructive interference, tune the directional far-field emission pattern, and affect the single-mode emission properties. The high reflectance of the embedded DBR structure can provide a high-quality factor of the lasing peak in the VCSEL devices. For the embedded DBR structures, the epitaxial AlGaIn/GaN [3,4], AlN/GaN [5], and AlInN/GaN [6] DBR structures have been reported that have high reflectivity at the emission wavelength region of the InGaIn active layers. All dielectric DBR VCSEL structures have been reported that are deposited on curved mirror of the sapphire substrate [7], on GaN after sapphire lift-off process [8], and as the epitaxial lateral overgrowth mirror [9]. The GaN VCSEL structure with bottom dielectric DBR and top TiO₂ high-index-contrast grating reflectors had been reported [10]. High efficiency InGaIn VCSELs had been reported with the conductive AlInN/GaN DBR structures [11–14]. For the current injection process, the VCSEL structure with buried tunnel junction had been demonstrated in the semi-polar blue GaN-based VCSEL [15]. The airgap DBR structure [16,17] was incorporated into the VCSEL fabrication because of a high refractive index contrast between GaN and airgap in the stack structure. As for the epitaxial DBR structure, a large lattice mismatch and lengthy epitaxial growth time are the challenges to be solved. The porous-GaN/GaN stack structure with short epitaxial growth time and large refractive index difference had been reported as the DBR structures [18–21] that were fabricated through a simple wet etching process. The lasing properties of the InGaIn VCSELs with the porous-GaN DBR structures were reported [22,23]. The mechanical [24], thermal [25], and electrical [23] properties of the InGaIn devices with porous structures have been reported. The InGaIn-based LED consisted of a 6λ cavity length and an embedded nanoporous DBR structure, without the top DBR structure, were reported in our previous report [26]. The single-mode and low threshold current density of the VCSEL devices can be realized in short 1λ resonant-cavity length. In the GaN-based VCSEL structure, 1λ cavity length is difficult to realize due to the large strain and the conductivity in the conventional AlGaIn- and AlN-based DBR structures. A 1.5λ -cavity GaN-based vertical-cavity surface-emitting laser has been reported by using the n-type conducting AlInN/GaN DBR structure [11].

In this paper, the optical confinement properties of 1λ InGaIn resonant-cavity light-emitting diode (RC-LED) structure was studied by adding the top dielectric distributed Bragg reflector (DBR) and the bottom porous-DBR structure. Through the epitaxial growth and electrochemical wet etching processes, the InGaIn active layer with an embedded 20-period porous-GaN/n-GaN DBR structure was demonstrated. Then, a Ta₂O₅ spacer layer as a cavity length adjustable layer and 8.5-period Ta₂O₅/SiO₂ alternately stacked structure for top reflector were deposited on the InGaIn epitaxial structure. The optical pumped lasing phenomenon at 432 nm was observed in the InGaIn resonant cavity with 1λ effective cavity length by tuning the thickness of Ta₂O₅ spacer layer. The surface morphology and optical properties of the InGaIn resonant-cavity structures were analyzed in detail.

2. Materials and Methods

InGaIn RC-LED structures were grown on a 4 in. c-face (0001) patterned sapphire substrate by using the metal-organic chemical vapor deposition (MOCVD) system. Trimethylgallium (TMGa), ammonia (NH₃) gas, and trimethylindium (TMIn) were used as gallium (Ga), nitrogen (N), and indium (In) sources material, respectively. Silane (SiH₄) and bis-cyclopentadienyl magnesium (CP2Mg) were used as the n-type and p-type doping sources, respectively. The LED epitaxial layers consisted of a 30 nm-thick GaN buffer layer, a 4.0 μm -thick unintentionally doped GaN layer, 20-period n⁺-GaIn:Si/n-GaN:Si (55 nm/45 nm) stacked structure, a 38 nm-thick n-GaN layer, 5-period In_{0.2}GaN/GaN (3 nm/9 nm) multiple-quantum wells (MQWs) structure, and a 50 nm-thick p-GaN layer. The growth temperatures of the GaN buffer layer and the u-GaN layer were measured at 530 °C and 1050 °C, respectively. The Si-doping concentrations of the stacked structure were measured at $2 \times 10^{19} \text{ cm}^{-3}$ for the n⁺-GaIn:Si layer and at $2 \times 10^{18} \text{ cm}^{-3}$ for the

n-GaN:Si layer, respectively, at 1050 °C. The growth temperature and Si-doping concentration of the n-GaN layer were measured at 1050 °C and $2 \times 10^{18} \text{ cm}^{-3}$, respectively. The growth temperature of the InGaN/GaN MQW active layer was measured at 760 °C. The growth temperature and Mg-doping concentration of the p-GaN layer were measured at 950 °C and $1 \times 10^{18} \text{ cm}^{-3}$, respectively. The p-type GaN:Mg layers were thermally activated in the furnace at 750 °C for 30 min in N_2 ambient gas. The lateral wet etching channels with a spacing of 230 μm on the LED structure were defined through the laser scribing (LS) process. The depth of LS line was measured at 2.2 μm to reach the as-grown 20-period n^+ -GaN:Si/n-GaN stacked structure by using 355 nm pulsed laser. The Indium metal contact was used to contact the n^+ -GaN:Si layer to apply the positive bias during the wet etching process. Then, the samples were cleaned through the ultrasonic cleaning process in the deionized water and the isopropyl alcohol (IPA) solution to remove the contamination in the etching channels. After the wet etching process, the n^+ -GaN:Si layers were transformed into porous GaN layers through the doping-selective electrochemical etching process in a 0.5 M nitride acid solution with a positive 8 V external bias voltage. The EC-treated samples were rinsed in the deionized water and dried for the following measurements. The GaN EC etching porosification chemistry/process have been reported [16,27]. Then, high refractive index n^+ -GaN:Si layers were transformed into low refractive index of porous GaN layers. The treated DBR structure consisted of a quarter-wavelength porous GaN layers and a quarter-wavelength GaN layers acted as a bottom reflector. Then, a 30 nm-thick Ta_2O_5 film was deposited on the top of the p-type GaN:Mg layer acting as a spacer layer for tuning the cavity length in the resonant-cavity structure. Finally, the 8.5-period $\text{Ta}_2\text{O}_5/\text{SiO}_2$ dielectric DBR was deposited onto the Ta_2O_5 spacer layer to complete the full RC-LED structure for optical measurement. The non-treated LED structure was defined as the standard LED (ST-LED). The InGaN LED with top and bottom DBR structure was defined as the resonant cavity LED (RC-LED). The photoluminescence spectra were measured by using monochromators (JOBIN YVON iHR550) with a TE-cooled charge-coupled device (CCD) detector. The surface morphologies of the RC-LED structures were observed using the optical microscope (OM) and the field-emission scanning electron microscope (FE-SEM, JEOL 6700F).

3. Results

In Figure 1a, the bottom porous-GaN/n-GaN DBR with blue light image and the laser scribing lines were observed by using optical microscope. The porous-DBR stacked structure consisted of a 55 nm thick, porous-GaN layer and a 45 nm thick GaN layer approximately in the cross-sectional SEM micrograph as shown in Figure 1b. The etching interface of the porous-GaN/n-GaN stack structure was observed clearly after the doping-selective electrochemical wet etching process. The 148 nm-thick LED structure with the InGaN MQW layers was shown in Figure 1c as the epitaxial cavity structure above the porous DBR structure. In our previous reports [19], the InGaN-based LED consisted of a large cavity length and an embedded nanoporous DBR structure without capping the top dielectric DBR structure. In this study, the 30 nm-thick Ta_2O_5 spacer layer and 8.5-period $\text{Ta}_2\text{O}_5/\text{SiO}_2$ dielectric DBR were deposited on the LED epitaxial layer as shown in Figure 1d. The resonant cavity consisted of the epitaxial InGaN active layer and the deposited Ta_2O_5 spacer layer between top dielectric DBR and bottom porous DBR structures.

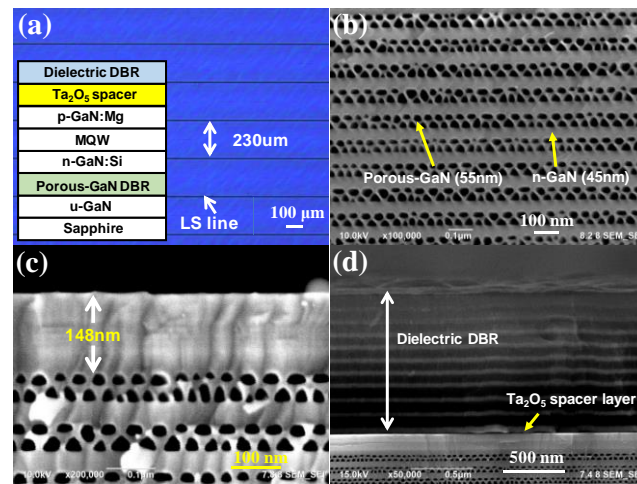


Figure 1. (a) The OM image of the InGaN LED with bottom porous-GaN DBR structure was observed with a blue reflected light image. (b) The cross-sectional SEM micrograph of the porous- distributed Bragg reflector (DBR) structure was observed. (c) A 148 nm thick InGaN LED structure was shown above the porous reflector. (d) The top reflector consisted of a 30 nm thick Ta₂O₅ spacer layer and a top Ta₂O₅/SiO₂ DBR structure.

In Figure 2, the reflectance spectra of the top Ta₂O₅/SiO₂ dielectric DBR and the bottom porous-GaN/n-GaN DBR structure were measured by using Xe lamp as a reference light source. The central wavelength, reflectivity, and the stopband width of the reflectance spectra were measured at 421.3 nm/98.1%/67 nm for the top dielectric DBR and at 434.3 nm/98.5%/55 nm for the porous DBR, respectively, listed in Table 1. The stopband width of the reflector is defined as the wavelength region that the reflectivity is higher than 90%. High reflectance and wide stopband width were observed on the top dielectric DBR and the bottom porous DBR structures.

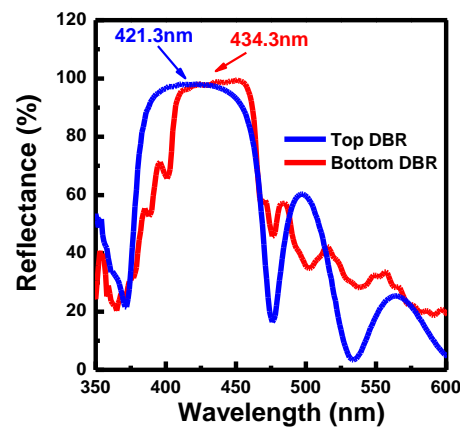


Figure 2. Reflectance spectra of top dielectric DBR and bottom porous-GaN DBR were measured at room temperature.

Table 1. Top and bottom DBR structures.

	Wavelength	Reflectivity	Stopband Width
Top dielectric DBR	421.3 nm	98.1%	67 nm
Bottom porous DBR	434.3 nm	98.5%	55 nm

As per Figure 3, the photoluminescence (PL) spectra were measured through angle-resolved measurement with a 405 nm laser source. When the incident 405 nm laser illu-

minated from the backside of the LED samples, the laser light will not be absorbed by the sapphire substrate, the n-type GaN:Si layer, and the p-type GaN:Mg layer at a normal direction. Only the InGaN active layers were excited and emitted the photoluminescence for the angle-resolved PL measurement. Then, the PL emission spectra were measured from the front-side of the LED chips.

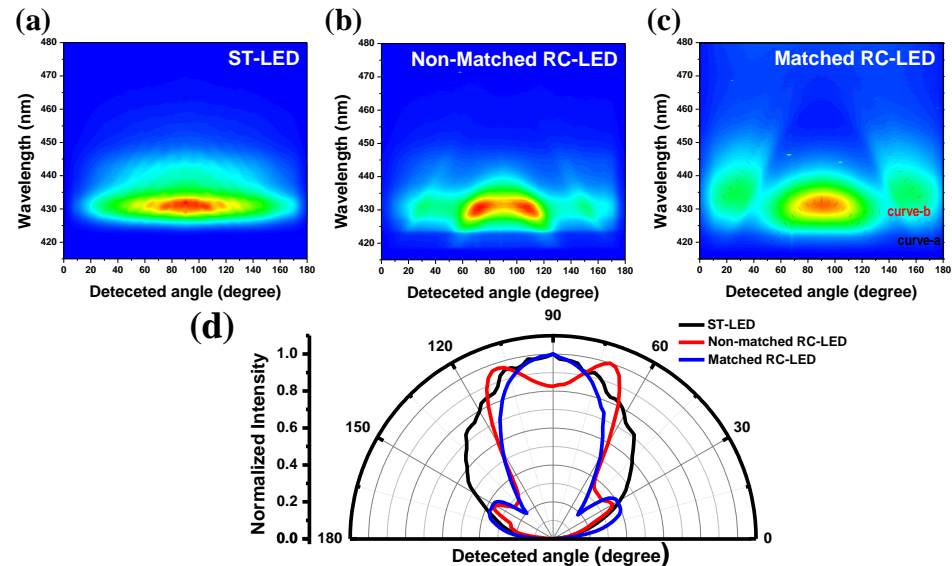


Figure 3. The photoluminescence (PL) emission spectra of (a) the ST-LED, (b) the non-matched RC-LED, and (c) the matched RC-LED were measured through the angle-resolved PL measurement. (d) Normalized far-field radiation patterns of all LED structures were measured.

In Figure 3a, the Fabry–Pérot (FP) interference line patterns of the non-treated LED (ST-LED) structure were observed with multiple curves due to the light reflected at the flat top GaN:Mg/Air interface and the bottom GaN/Al₂O₃ interface. The thickness of the epitaxial layers was calculated as the value of 6.1 μm for the ST-LED, which was similar to the actual epitaxial thickness grown on sapphire substrate. In non-matched RC-LED structure, 8.5-period Ta₂O₅/SiO₂ dielectric DBR layers were deposited on the LED structure directly without a spacer layer. The peak intensities of the far-field pattern measured at 72° and 108° detected angles that were higher than it at normal direction (90°) as shown in Figure 3b. As for the matched RC-LED structure with 30 nm-thick Ta₂O₅ spacer layer, the two interference line patterns were observed apparently in the far-field PL spectra. The PL emission wavelength of the InGaN active layer was matched to the interference curve in the far-field PL spectra pattern as shown in Figure 3c. The intensity formula of the angle-resolved spectra was $I(\lambda_0, \theta) = (2n_s T / m_c) \cos(\theta) = \lambda_0 \cos(\theta)$, where n_s is the refractive index of GaN (2.48), m_c is the cavity mode number, and T represents the cavity thickness [26]. In Figure 3c, the simulated interference line pattern was matched to the peak emission wavelength of the InGaN active layer. The fitting thickness of the InGaN LED cavity structure was calculated as the value of 173 nm between the bottom porous DBR and the top dielectric DBR structure. The FP second order mode in the 1λ resonant cavity was matched to the PL emission wavelength of the InGaN active layer as shown in curve-a in Figure 3c. From the simulation results, the penetration depths were calculated as the value of 196 nm-thick for the bottom porous DBR and 138 nm-thick for the top dielectric DBR. The effective cavity length in curve-b consisted of the 148 nm-thick InGaN active layer, 30 nm-thick Ta₂O₅ spacer layer, the 196 nm-thick penetration depth of the porous DBR, and 138 nm-thick penetration depth of the dielectric DBR as shown in Figure 3c. The normalized PL intensity of the far-field radiation patterns of all LED structures were measured in Figure 3d. By forming the resonant-cavity structure, the divergent angle was drastically decreased from 114° for the ST-LED to 57° for the matched RC-LED structure.

The peak emission intensity of the matched RC-LED structure was observed at normal direction (90°) that matched to the resonant cavity length between top dielectric and bottom porous DBR structures.

In Figure 4, the optical pumping spectra of the InGaN resonant cavity structure were measured by using a Nd:YVO₄ 355 nm pulsed laser as laser excitation source. In Figure 4a, the PL peak intensities and the linewidth of the PL spectra were measured as a function of the laser excited power. By increasing the laser pumping power, the PL emission intensities had a non-linear increasing property. The threshold value of the laser pumping power (P_{th}) was measured as the value of 14.8 μ W at room temperature. In the matched RC-LED structure, the linewidth of the PL spectra was reduced from 6.5 nm to 0.7 nm by increasing the laser pumping power. In Figure 4b, the PL emission spectra of the matched RC-LED structure were observed under $0.95 P_{th}$, $1.02 P_{th}$, and $1.05 P_{th}$ laser pumping power, respectively. The linewidth and dominated emission wavelength of the InGaN active layer were measured at 6.5 nm for the spontaneous emission peak (at 431.3 nm) and at 0.7 nm for the stimulated emission peak (at 431.8 nm). The lasing phenomenon of the matched InGaN resonant cavity structure was measured at 431.8 nm with a 0.7 nm linewidth at room temperature.

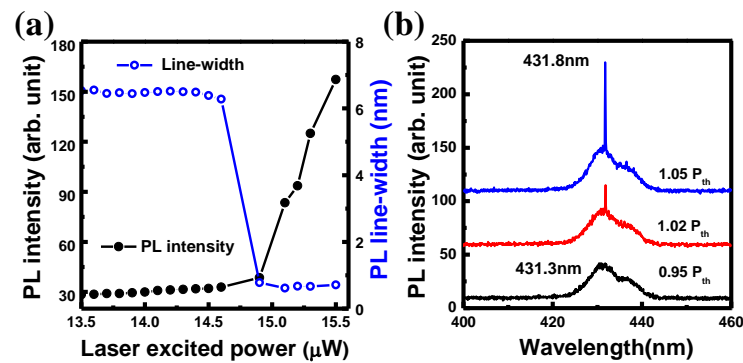


Figure 4. (a) The PL intensities and the linewidth of the optical pumping spectra were measured as a function of the laser excited power. (b) The emission spectra of the RC-LED structure were observed under $0.95 P_{th}$, $1.02 P_{th}$, and $1.05 P_{th}$ laser pumping power.

4. Conclusions

In summary, InGaN RC-LED structures with bottom porous DBR and top dielectric DBR structures were fabricated. The directional PL emission phenomenon at normal direction was observed by tuning the Ta₂O₅ spacer layer to match the 1λ cavity length in the resonant cavity structure. The short cavity and single mode emission of the InGaN resonant cavity structure can be realized by using the embedded EC-treated porous-GaN/n-GaN DBR structure. A small divergent angle and a narrow linewidth of the PL spectra were observed in the InGaN RC-LEDs which have the potential for the projective light source and the VCSEL applications.

Author Contributions: Formal experiment and analysis, C.-J.W., Y.K., G.-Y.S., Y.-Y.C.; data curation, Y.-S.L., H.C.; writing—review and editing, C.-F.L. All authors have read and agreed to the published version of the manuscript.

Funding: Ministry of Science and Technology of Taiwan under grant No. 108-2221-E-005 -064 and 108-2221-E-005 -035 -MY2.

Data Availability Statement: Please refer to suggested Data Availability Statements in section “MDPI Research Data Policies” at <https://www.mdpi.com/ethics>.

Acknowledgments: The authors gratefully acknowledge the support from the Innovation and Development Center of Sustainable Agriculture’s Featured Areas Research Center Program within the framework of Taiwan’s Ministry of Education’s Higher Education Sprout Project.

Conflicts of Interest: The authors declare no conflict of interest.

References

1. Someya, T.; Werner, R.; Forchel, A.; Catalano, M.; Cingolani, R.; Arakawa, Y. Room Temperature Lasing at Blue Wavelengths in Gallium Nitride Microcavities. *Science* **1999**, *285*, 1905–1906. [[CrossRef](#)]
2. Liu, A.; Wolf, P.; Lott, J.A.; Bimberg, D. Vertical-cavity surface-emitting lasers for data communication and sensing. *Photonics Res.* **2019**, *7*, 121–136. [[CrossRef](#)]
3. Nakada, N.; Nakaji, M.; Ishikawa, H.; Egawa, T.; Umeno, M.; Jimbo, T. Improved Characteristics of InGaN Multiple-Quantum-Well Light-Emitting Diode by GaN/AlGaIn Distributed Bragg Reflector Grown on Sapphire. *Appl. Phys. Lett.* **2000**, *76*, 1804–1806. [[CrossRef](#)]
4. Lin, C.F.; Yao, H.H.; Lu, J.W.; Hsieh, Y.L.; Kuo, H.C.; Wang, S.C. Characteristics of Stable Emission GaN-Based Resonant-Cavity Light-Emitting Diodes. *J. Cryst. Growth* **2004**, *261*, 359–363. [[CrossRef](#)]
5. Carlin, J.F.; Ilegems, M. High-Quality AllnN for High Index Contrast Bragg Mirrors Lattice Matched to GaN. *Appl. Phys. Lett.* **2003**, *83*, 668–670. [[CrossRef](#)]
6. Hamaguchi, T.; Nakajima, H.; Tanaka, M.; Ito, M.; Ohara, M.; Jyoukawa, T.; Kobayashi, N.; Matou, T.; Hayashi, K.; Watanabe, H.; et al. Sub-milliamperre-threshold continuous wave operation of GaN-based vertical-cavity surface-emitting laser with lateral optical confinement by curved mirror. *Appl. Phys. Express* **2019**, *12*, 044004. [[CrossRef](#)]
7. Higuchi, Y.; Omae, K.; Matsumura, H.; Mukai, T. Room-Temperature CW Lasing of a GaN-Based Vertical-Cavity Surface-Emitting Laser by Current Injection. *Appl. Phys. Express* **2008**, *1*, 121102. [[CrossRef](#)]
8. Leonard, J.T.; Yonkee, B.P.; Cohen, D.A.; Megalini, L.; Lee, S.; Speck, J.S.; DenBaars, S.P.; Nakamura, S. Nonpolar III-nitride vertical-cavity surface-emitting laser with a photoelectrochemically etched air-gap aperture. *Appl. Phys. Lett.* **2016**, *108*, 031111. [[CrossRef](#)]
9. Hamaguchi, T.; Tanaka, M.; Mitomo, J.; Nakajima, H.; Ito, M.; Ohara, M.; Kobayashi, N.; Fujii, K.; Watanabe, H.; Satou, S.; et al. Lateral carrier confinement of GaN-based vertical-cavity surface-emitting diodes using boron ion implantation. *Jpn. J. Appl. Phys.* **2016**, *55*, 122101. [[CrossRef](#)]
10. Chang, T.C.; Hashemi, E.; Hong, K.B.; Bengtsson, J.; Gustavsson, J.; Haglund, A.; Lu, T.C. Electrically Injected GaN-Based Vertical-Cavity Surface-Emitting Lasers with TiO₂ High-Index-Contrast Grating Reflectors. *ACS Photonics* **2020**, *7*, 861–866. [[CrossRef](#)]
11. Ikeyama, K.; Kozuka, Y.; Matsui, K.; Yoshida, S.; Akagi, T.; Akatsuka, Y.; Koide, N.; Takeuchi, T.; Kamiyama, S.; Iwaya, M.; et al. Room-temperature continuous-wave operation of GaN-based vertical-cavity surface-emitting lasers with n-type conducting AllnN/GaN distributed Bragg reflectors. *Appl. Phys. Express* **2016**, *9*, 102101. [[CrossRef](#)]
12. Muranaga, W.; Akagi, T.; Fuwa, R.; Yoshida, S.; Ogimoto, J.; Akatsuka, Y.; Iwayama, S.; Takeuchi, T.; Kamiyama, S.; Iwaya, M. GaN-based vertical-cavity surface-emitting lasers using n-type conductive AllnN/GaN bottom distributed Bragg reflectors with graded interfaces. *Jpn. J. Appl. Phys.* **2019**, *58*, SCCC01. [[CrossRef](#)]
13. Kuramoto, M.; Kobayashi, S.; Akagi, T.; Tazawa, K.; Tanaka, K.; Saito, T.; Takeuchi, T. High-power GaN-based vertical-cavity surface-emitting lasers with AllnN/GaN distributed Bragg reflectors. *Appl. Sci.* **2019**, *9*, 416. [[CrossRef](#)]
14. Iida, R.; Ueshima, Y.; Muranaga, W.; Iwayama, S.; Takeuchi, T.; Kamiyama, S.; Iwaya, M.; Akasaki, I. GaN-based vertical cavity surface emitting lasers with lateral optical confinements and conducting distributed Bragg reflectors. *Jpn. J. Appl. Phys.* **2020**, *59*, SGGE08. [[CrossRef](#)]
15. Kearns, J.A.; Back, J.; Palmquist, N.C.; Cohen, D.A.; DenBaars, S.P.; Nakamura, S. Inhomogeneous Current Injection and Filamentary Lasing of Semipolar (20-2-1) Blue GaN-Based Vertical-Cavity Surface-Emitting Lasers with Buried Tunnel Junctions. *Phys. Status Solidi Appl. Mater. Sci.* **2019**, *217*, 1900718. [[CrossRef](#)]
16. Chen, D.; Han, J. High reflectance membrane-based distributed Bragg reflectors for GaN photonics. *Appl. Phys. Lett.* **2012**, *101*, 221104. [[CrossRef](#)]
17. Tao, R.; Kamide, K.; Arita, M.; Kako, S.; Arakawa, Y. Room-temperature observation of trapped exciton-polariton emission in GaN/AlGaIn microcavities with Air-Gap/III-Nitride distributed Bragg reflectors. *ACS Photonics* **2016**, *3*, 1182–1187. [[CrossRef](#)]
18. Park, J.; Kang, J.H.; Ryu, S.W. High Diffuse Reflectivity of Nanoporous GaN Distributed Bragg Reflector Formed by Electrochemical Etching. *Appl. Phys. Express* **2013**, *6*, 072201. [[CrossRef](#)]
19. Shieh, B.C.; Jhang, Y.C.; Huang, K.P.; Huang, W.C.; Dai, J.J.; Lai, C.F.; Lin, C.F. InGaIn Light-Emitting Diodes with Embedded Nanoporous GaN Distributed Bragg Reflectors. *Appl. Phys. Express* **2015**, *8*, 082101. [[CrossRef](#)]
20. Zhang, C.; Park, S.H.; Chen, D.; Lin, D.W.; Xiong, W.; Kuo, H.C.; Lin, C.F.; Cao, H.; Han, J. Mesoporous GaN for Photonic Engineering—Highly Reflective GaN Mirrors as an Example. *ACS Photonics* **2015**, *2*, 980–986. [[CrossRef](#)]
21. Fan, F.H.; Syu, Z.Y.; Wu, C.J.; Yang, Z.J.; Huang, B.S.; Wang, G.J.; Lin, Y.S.; Chen, H.; Kao, C.H.; Lin, C.F. Ultraviolet GaN Light-Emitting Diodes with Porous-AlGaIn Reflectors. *Sci. Rep.* **2017**, *7*, 4968. [[CrossRef](#)] [[PubMed](#)]
22. Masabih, S.M.M.U.; Aragon, A.A.; Monavarian, M.; Luk, T.S.; Feezell, D.F. Electrically injected nonpolar GaN-based VCSELs with lattice-matched nanoporous distributed Bragg reflector mirrors. *Appl. Phys. Express* **2019**, *12*, 036504. [[CrossRef](#)]
23. Elafandy, R.T.; Kang, J.H.; Li, B.; Kim, T.K.; Kwak, J.S.; Han, J. Room-temperature operation of c-plane GaN vertical cavity surface emitting laser on conductive nanoporous distributed Bragg reflector. *Appl. Phys. Lett.* **2020**, *117*, 011101. [[CrossRef](#)]
24. Wu, C.J.; Chen, Y.Y.; Wang, C.J.; Shiu, G.Y.; Huang, C.H.; Liu, H.J.; Chen, H.; Lin, Y.S.; Lin, C.F.; Han, J. Anisotropic properties of pipe-GaN distributed Bragg reflectors. *Nanoscale Adv.* **2020**, *2*, 1726–1732. [[CrossRef](#)]

25. Zhou, T.; Zhang, C.; ElAfandy, R.; Yuan, G.; Deng, Z.; Xiong, K.; Chen, F.M.; Kuo, Y.K.; Xu, K.; Han, J. Thermal transport of nanoporous gallium nitride for photonic applications. *J. Appl. Phys.* **2019**, *125*, 155106. [[CrossRef](#)]
26. Lai, C.F.; Kuo, H.C.; Chao, C.H.; Yu, P.; Yeh, W.Y. Structural Effects on Highly Directional Far-Field Emission Patterns of GaN-Based Micro-Cavity Light-Emitting Diodes with Photonic Crystals. *J. Lightwave Technol.* **2010**, *28*, 2881–2889. [[CrossRef](#)]
27. Pasayat, S.S.; Ley, R.; Gupta, C.; Wong, M.S.; Lynsky, C.; Wang, Y.; Gordon, M.J.; Nakamura, S.; Denbaars, S.P.; Keller, S.; et al. Color-tunable <10um square InGaN micro-LEDs on compliant GaN-on-porous-GaN pseudo-substrates. *Appl. Phys. Lett.* **2020**, *117*, 061105.